

Space Time Recurrent Memory Network

Hung Nguyen, Fuxin Li
Oregon State University

{nguyehu5, lif}@oregonstate.edu

Abstract

We propose a novel visual memory network architecture for the learning and inference problem in the spatial-temporal domain. Different from the popular transformers, we maintain a fixed set of memory slots in our memory network and explore designs to input new information into the memory, combine the information in different memory slots and decide when to discard old memory slots. Finally, this architecture is benchmarked on the video object segmentation and video prediction problems. Through the experiments, we show that our memory architecture can achieve competitive results with state-of-the-art while maintaining constant memory capacity.

1. Introduction

Video Object Segmentation (VOS) is a fundamental vision problem and has gained increasing attention in recent years. VOS has many applications including video matting, augmented reality, automatic driving, etc. Depending on the supervision level, VOS can be categorized into sub tasks: unsupervised (zero-shot), semi-supervised (one-shot), and interactive VOS. In the most popular semi-supervised setting, each video provides masks for objects of interest in the first frame the object appears. The algorithm needs to segment those objects in the remaining of the video and maintains correct identities.

Video object segmentation is a difficult problem since objects often exhibit multiple appearances, can deform in a non-rigid manner, and a small error, e.g. a piece of background mistakenly included in the foreground, could possibly drift to significant errors as the piece grows in size. Hence, it is a very nice test ground for spatio-temporal deep learning models. A successful spatio-temporal network model would have to remember multiple diverse appearances of each object, precisely decide to remember and forget specific regions in order to achieve optimal performance.

Currently, the top-performing algorithms on this task are mainly attention-based models [20]. The model structures

are similar to transformers used in natural language processing where they compute attention maps (referred to as keys) from the current frame to each of the previous frames and use a weighted average of the features (referred to as values) of the previous frames based on the attention map to guide the segmentation on the current frame. However, videos are different from natural language in that each frame consists of substantial information and subsequent frames are mostly similar, as opposed to natural language where each word contains less information but are usually different from one another. In video, storing the key/value pairs from each frame is prohibitive in terms of memory requirement. Visual recognition also could involve much longer sequences than NLP, as it is not uncommon for sequences to contain hundreds or thousands of frames. The storage requirement in transformers is prohibitive if we consider running them in such long sequences. In practice, heuristics such as sampling every fifth frame are usually utilized [20], but it does not fundamentally address the linear increase in memory requirement w.r.t. sequence length.

Our goal in this paper is to explore an approach where the memory size is kept constant. Namely, we aim to have a fixed number of memory blocks, which can be considered as templates for the target object. Each template contains the information about the object at a particular pose. Instead of heuristically as in prior work, we would attempt to update this memory automatically, which poses new challenges to the model: this new memory model needs to properly aggregate the information from multiple frames, deciding information from which frames needs to be merged and how to merge them. Since the number of templates is fixed, our model also needs to understand when to discard previously remembered templates. Hence, the network design is significantly more challenging than transformer networks. Yet, we believe that this kind of memory structure has more potential to scale up to long videos beyond a few seconds, and touches upon more fundamental challenges in memory organization that would be potentially valuable to problems far beyond video object segmentation. Besides, it is arguable that intelligent beings, no matter humans or machines, should have an approach to organize their mem-

ory rather than simply let it grow linearly w.r.t. the length of the spatio-temporal sequence they have seen. In the paper we explore multiple different design choices which shed light on the designs of such a memory network applied to a practical problem such as VOS.

Our contributions can be summarized as follows:

- We introduce a novel memory network which has a constant number of slots, that can handle a long sequence of images efficiently without increasing the size of the memory when the length of the video grows.
- We explore several different memory update rules for the aggregation of information from multiple memory slots.
- Experiments show that our model is able to summarize and compress past information into a constant-size memory. With our memory network that adopts constant-size memory, we are able to match state-of-the-art performance of transformer-based models on the VOS task and outperform other methods on video prediction task.

2. Related Work

Implicit Memory. Long short-term memory (LSTM) [7] improves the vanilla recurrent networks (RNN) by maintaining an inner self-loop of the cell state, which allows the cell state to stay constant if there is no additional input. It also includes input and forget gates which allow information to be filtered before being used to update the memory. The Gated recurrent unit (GRU) simplifies the gates in LSTM by combining the input and forget gates. These gates are usually implemented with fully connected layers and hence cannot be applied to high dimensional data such as images. [24] resolved this issue by replacing the linear layers with convolutional layers instead. However, most of these architectures only have a single memory vector, which struggles to capture multiple appearances of objects in video reasoning problems [11].

Explicit Memory. Neural Turing Machine (NTM) [5] extended the traditional RNN with an external memory. This memory is detached from the main computational graph in the sense that unlike RNN/LSTM, changing the size of the memory does not affect the number of parameters of the model. NTM architecture includes a controller and a memory bank. These two components interact with each other through multiple read and write heads. The controller receives information, interacts with the memory through read and write heads to retrieve related information, removes the old information, and saves the new one if useful. Based on the retrieved information, a corresponding response is returned. However, it is non-trivial to scale

NTM’s memory for visual tasks which require spatial information such as segmentation. The main bottleneck of this architecture is the controller. This controller is usually implemented with sequential models such as vanilla RNN, GRU, or LSTM, which use fully-connected layers.

Space Time Memory network (STM). STM [20] can be considered as an explicit memory-based network without a memory controller. Each memory block or cell of STM contains a template for the objects to be segmented. Each template includes 2 components, key and value, that are responsible for retrieving the related information about the objects in query frames. In the reading stage, STM utilizes an operation called Space Time Memory read which essentially uses the attention mechanism to retrieve the attended feature for the target object from the memory. However, STM does not provide a mechanism to update the memory. Each template after generated is fixed. When a new template appears, it is simply concatenated with the old ones. One advantage of this simple mechanism is that the information on each template is not contaminated by other ones. However, choosing which template to keep is non trivial and can be tricky. STM uses a simple heuristic to add a new template every 5 frames. However, depending on the frame rate or how quick the target moves, this heuristic can be sub-optimal. Besides, since the old templates are not removed, the memory grows linearly w.r.t. the number of frames, which can be a significant issue.

Global context module (GC). GC [14] tries to address the linear memory growth rate in STM by proposing the Global Context module. The author replaces the key and value maps with a fixed-size context matrix C for each frame. The global context matrix G is the element-wise average of all past frames’ matrices C . The matrix G is the network’s memory and used to extract related information about target objects in the inference stage. The author proves that the global context module achieves the same representational power as that of STM. However, this property can only be achieved without any non-linear activation functions, which does not apply in the case of STM. Therefore, the performance of GC is significantly inferior to that of STM.

Episodic graph memory network (EGM). EGM [17] represents the memory as a fully connected graph with each node being a template. The model performs k steps reasoning using the memory with the query frame. This process allows the interaction among memory nodes with the query, and thus builds up a high order function of the nodes and the query. However, this model does not provide a proper way to update the memory. Given a new query frame, the model uses the first (i.e ground-truth) frame and previous segmented frame and samples $N - 2$ segmented frames from the support set including past segmented frames to re-initialize the memory. In other words, the memory is reset

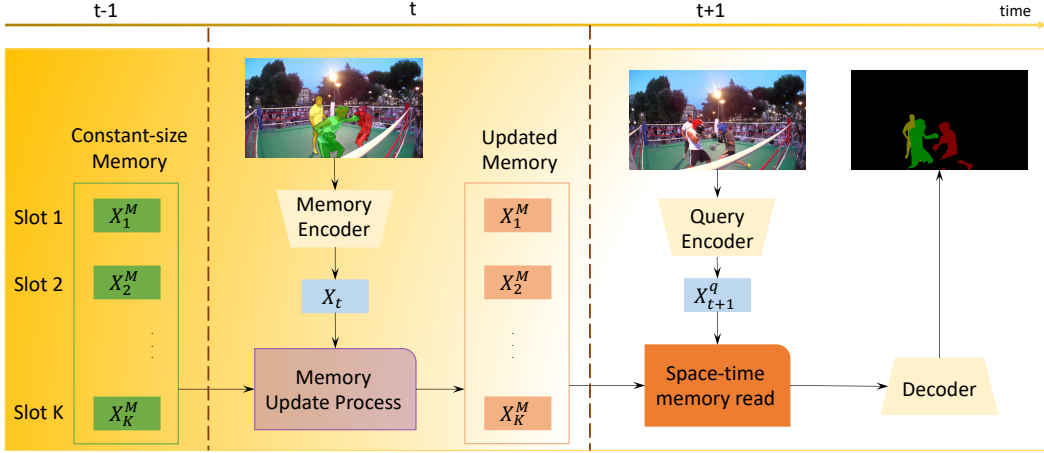


Figure 1. **The overview of our framework.** Assuming a constant-size memory with K slots, our framework includes 2 stages. **Memory Update:** in this stage, the network generates a new feature map X_t based on the current frame with the corresponding masks using the memory encoder. This feature map is then used to update the memory (Sec. 3.2). **Inference stage:** a feature map X_{t+1}^q is generated from the query image using the query encoder and goes through the space-time memory read module to access the memory and retrieve object-related information to create a new feature. This feature is finally decoded into our predicted mask (which will be then used to update the memory again). (Best viewed in color)

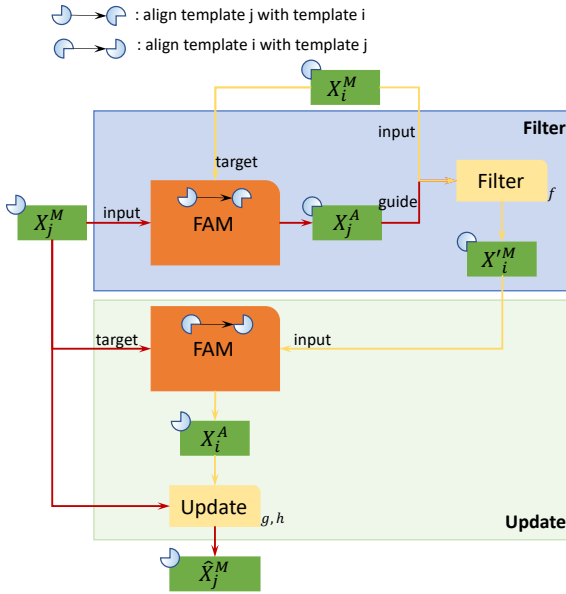


Figure 2. **Fusion Cell.** The Fusion Cell is used to distill information from X_i^M to X_j^M using the FAM and gating function, Filter and Update.

each time making an inference. This behavior differs from other memory networks which usually have an aggregation function allowing new information to be easily inserted into the memory. Besides, resetting the memory too frequently will throw away valuable information built up from previous reasoning steps. Another disadvantage is that there

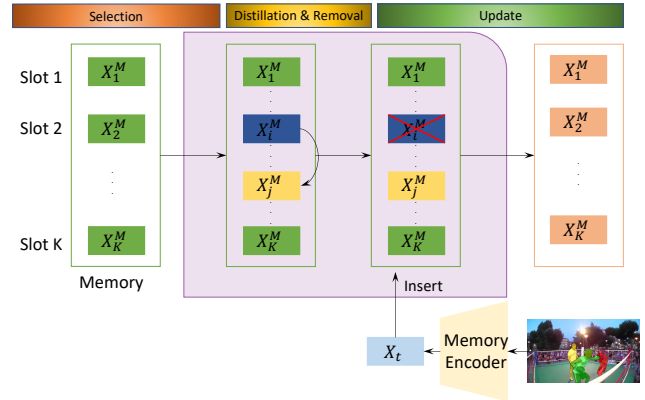


Figure 3. **Memory Update Process.** The update process includes 3 steps. **Selection step:** 2 templates, X_i^M and X_j^M where $i < j$, are chosen from the memory based on their similarity. **Distillation & Removal step:** the information from X_i^M is distilled into X_j^M using the Fusion Cell, and X_i^M is purged from the memory. **Update step:** a template X_t is generated using our Memory Encoder and the current frame together with its extra information such as objects' masks, optical flow, or previous frames if needed. This template is added to the end of the memory (i.e after X_K^M).

are always exactly N different frames from the video in the memory at a time. Therefore, when the video gets longer, the memory can miss lots of important information.

Online vs Offline learning in Video Object Segmentation. In video object segmentation, the online methods [21, 3, 27, 2, 1, 13, 8, 22] utilize data augmentation on the first frame with ground truth or middle frames with

their own predictions to fine-tune the baseline model, creating a different model for each video. These approaches, while produce accurate results, take a lot of time during the fine-tuning process and are unrealistic in practice. In contrast, offline methods fix their parameters after training and provide a different way to remember target object appearances.[20, 14, 23] maintain object appearances through an explicit memory. [35, 34, 19, 15] utilize the ground truth and the previous frames as a reference for their prediction. [35] performs the best due to their inclusion of multiple engineering tricks which are orthogonal to the contribution in our paper.

3. Methods

3.1. Overview

Our framework (Fig. 1) includes a Memory Encoder, a Query Encoder, a Decoder, and a fixed-size memory with K templates of the target object. These modules are used in 2 main stages: memory update and inference stages.

In the memory update stage (Section 3.2), the memory update process takes the memory from previous time step ($t-1$) and the encoded feature map (or called template) by feeding the current frame with its corresponding information (e.g object mask in the VOS problem) to the Memory Encoder (a CNN network) to generate a new memory.

In the inference stage, the Query Encoder takes the current frame to generate an encoded feature map X^q . It is similar but slightly different from the Memory Encoder in that it works on the image only and does not take additional information such as a segmented mask as input. The feature map of the target object is generated by densely matching every pixel in the X^q with every pixel in the memory templates through the space-time memory read mechanism (section 3.3). Finally, the attended feature is decoded into our final prediction with the decoder.

3.2. Memory Update Process

Our Memory Update Process is depicted in Fig. 3. Let K and n be the maximum number and the current number of slots in the memory. Each slot contains one template extracted from the video. If $n < K$, the new template is simply added to the memory. If $n = K$, then a template must be removed from the memory to create an empty slot for the new template. However, removing a template completely from the memory might be detrimental because the removed template might carry useful information that can only be observed in the corresponding frame. Hence, we want to distill the important information from the removed template to others. Besides, when the first frame is the ground truth and hence most reliable, it is useful to always keep that frame in the memory, which means $1 < i \leq K$. Otherwise, if we do not have the ground truth, then $1 \leq i \leq K$. We tested 4

different update rules:

- **A:** $i = 2$ and $J = \{3, \dots, n_{max}\}$: we remove the oldest template that is not the ground truth and use it to update the remaining templates .
- **B:** $i = n_{max}$ and $J = \{2, \dots, n_{max} - 1\}$: we choose the newest frame to remove and use it to update the remaining templates.
- **C:** We choose i and j such that $i < j \leq K$ and $(i, j) = \operatorname{argmin}_{i,j} S(X_i^M, X_j^M)$ where $S(X_i, X_j)$ is the similarity function between 2 templates. In other words, X_i^M and X_j^M is the least similar pair of template in the memory.
- **D:** We choose i and j such that $i < j \leq K$ and $(i, j) = \operatorname{argmax}_{i,j} S(X_i^M, X_j^M)$. In other words, X_i^M and X_j^M is the most similar pair of template in the memory.

The similarity function between 2 templates $X_i^M, X_j^M \in R^{HW \times d}$ is defined based on the many to one matching between the keys of 2 corresponding frames:

$$S(X_i^M, X_j^M) = \frac{1}{HW} \sum_p \max_q c(X_i^M(p), X_j^M(q)) \quad (1)$$

$$c(X_i^M(p), X_j^M(q)) = \frac{X_i^M(p)X_j^M(q)}{|X_i^M(p)||X_j^M(q)|} \quad (2)$$

where $X_i^M(p)$ extracts the feature at spatial location p . S is the average similarity between the most similar location pairs in X_i^M and X_j^M .

The Fusion cell (Fig. 2) is used to distill information from the removed template X_i^M to the target template X_j^M . This cell includes 2 stages: filter and update. In the filter stage, the noisy information is removed from X_i^M using X_j^M as our guide. To do that, X_j^M is aligned with X_i^M with an attention module named FAM:

$$FAM(X_i^M, X_i^M) = \operatorname{Softmax}(X_i^M(X_i^M)^T)X_i^M \quad (3)$$

After that, a gating function is applied to filter out unnecessary features from X_i^M . We describe step 1 as follows:

$$X_j^A = FAM(X_i^M, x_j^M) \quad (4)$$

$$r = \sigma(f([X_i^M, X_j^A])) \quad (5)$$

$$X_i'^M = r \odot X_i^M \quad (6)$$

where f is implemented with CNN, σ is the sigmoid function, and \odot is the Hadamard product.

This stage is important because we use our prediction, which is noisy, in addition to the corresponding frame to

extract the template. The filter step helps to remove the noisy information from the template before actually using it to update X_j^M . In the update stage, X_i^M is aligned with X_j^M to create a potential template, X_i^A . Then X_i^A is used to update template X_j^M as follows:

$$X_i^A = FAM(X_j^M, X_i^M) \quad (7)$$

$$z = \sigma(h([X_i^A, X_j^M])) \quad (8)$$

$$n = \tanh(g([X_i^A, X_j^M])) \quad (9)$$

$$\hat{X}_j^M = (1 - z) \odot X_j^M + z \odot n \quad (10)$$

where h , and g are implemented using CNN.

Note that in our framework, the update process happens among templates within the memory. The newest template is only copied to the memory after the update process takes place and does not directly interfere with that process. This property makes our model different from memory modules such as LSTM [7] or Neural Turing Machine [5]. Specifically, let $Mem = \{X_1^M, X_2^M, \dots, X_K^M\}$ be the memory of our network and X_t be the template of the newest frame. LSTM and NTM update formulae are functions between the new input and the current memory:

$$X_{i,t}^M = G(X_{i,t-1}^M, X_t) \quad (11)$$

for all $1 \leq i \leq n$. However, instead of X_t we use another memory cell:

$$X_{i,t}^M = G(X_{i,t-1}^M, X_{j,t-1}^M) \quad (12)$$

and keep the new template X_t intact in the memory. This modification allows the reasoning within the memory and create higher order interaction among memory cells while the new template is kept intact. This behavior conforms with our argument that when receiving a new information, human mind would keep it fresh for a period of time before blending it with the long term information to solidify our memory and build up the knowledge base about the world. In section 4.1.3 we show ablation experiments comparing these two approaches.

3.3. Inference Stage

In the inference stage, the query frames goes through the Query Encoder to be encoded into a feature map and converted into a key-value pair (k^q, v^q) in the space-time memory module (Fig. 4). Similarly, each template in the memory is converted into a key-value pair and all templates are concatenated to form (k^M, q^M) . Unlike k^q and v^q which only contain information from query frames, k^M and q^M carry information of every frame in the past that is condensed into a fixed number (i.e K) of templates in the memory thanks to our Memory Update Process module. Then each pixel i of

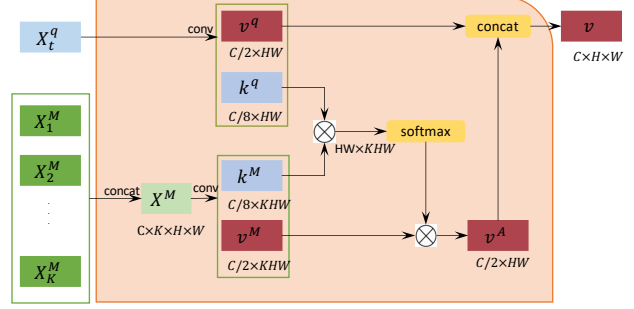


Figure 4. **Space-time memory module** - adapted from VOSSTM[20].

the query template is densely matched with every pixel j of memory's templates through the attention mechanism [20]:

$$y_i = \left[\frac{1}{\sum_j \exp(k_i^q \cdot k_j^M)} \exp(k_i^q \cdot k_j^M) v_j^M, v_i^q \right] \quad (13)$$

where $1 \leq i \leq HW$, $1 \leq j \leq KHW$, and $[\cdot, \cdot]$ is the concatenation. y is then decoded into the segmentation mask.

3.4. Implementation and Training Details

3.4.1 Implementation

The architectures of the encoder and decoder are the same as those of [20]. However, we replace batch normalization [9] layers with group normalization [32] in our backbone - Resnet 50. This made the training more stable because of the small batch size due to memory constraints. The network uses 5 memory blocks including: 1 block for the ground truth (1st frame), 1 block for the latest frame, and 3 blocks for intermediate frames. Post processing was also employed to remove some false positive predictions that are far away from the object in the previous frame.

3.4.2 Training

The model is trained in 2 stages: pretraining with images and fine-tuning with videos.

- **Pre-training stage.** We use images from image segmentation datasets including COCO [16], ECSSD [33], SBD [6], MSRA10k [4], and HKUIS [12]. Each image is then augmented to simulate a short video of 5 frames. The maximum number of objects within each video is set to 4 (including background). We use Cross Entropy loss and Adam optimizer with initial learning rate set to 10^{-4} . The learning rate is dropped by a factor of 0.1 each time the error on validation set, which is created from images in the validation sets of corresponding datasets, does not decrease.

- **Fine-tuning stage.** Each training sample is composed of 50 continuous frames from each video of DAVIS. Each frame is further augmented with linear transformation and color jittering. The model is trained in truncated backpropagation through time setting where each segment includes 10 frames.

The resolution of the video in both the pre-training and the fine-tuning stages is 384×384 .

4. Experiments

4.1. Video object segmentation

The VOS dataset is chosen to benchmark our proposed memory network for the following reasons:

- VOS requires both long and short term memory to segment the objects efficiently.
- The variation of appearance of the object throughout the video is large. This property requires the network to keep a diverse memory.
- The segmentation task requires the network to preserve a huge number of details (i.e. feature maps instead of a vector), the fact that usually requires tremendous amount of computational resources in other memory networks.

4.1.1 DAVIS

The DAVIS dataset is one of the primary datasets for VOS task. There are 2 versions: single object - DAVIS 2016 and multiple objects - DAVIS 2017. DAVIS 2016 includes 30 videos in training set and 20 videos in validation set. DAVIS 2017 includes 60 videos, 30 videos, and 30 videos in the training, validation, and test-dev sets respectively. The author provided 2 sets of datasets with different resolution (i.e. 480p vs 780p). The maximum number of objects in each video is 11. The objects range from common classes such as human or dog to rare classes such as string, car wheel, and drone. The number of frames in each video can be more than 100.

Table 1 shows the quantitative result of our method in comparison with others on the DAVIS 2017 validation set. Our result outperforms most other approaches when trained only on DAVIS, including approaches with and without online fine tuning. On the test-dev set, we achieve results close to PRemVOS which included online fine tuning. Among models that only use DAVIS to fine-tune, our model outperforms them by several points, both in J & F. More results on DAVIS is shown in the supplementary material.

4.1.2 Youtube VOS

Youtube VOS is the largest dataset for video object segmentation task. We test our model on the Youtube 2018 version. This dataset includes more than 4000 videos which includes 94 type of objects' categories such as human, animal, or vehicles. The validation set includes 474 videos including 65 seen categories and 26 unseen categories that cover 894 object instances. Unlike objects in DAVIS dataset, objects in Youtube can appear in the middle of the video. Because our model maintain separate memory for each object, this change does not impact significantly to the performance. Tab. 2 shows our result on Youtube 2018. Our model only fine-tuned on the DAVIS dataset significantly outperforms STM on YouTube. Our model fine-tuned on the YouTube dataset is competitive among memory-based methods. Especially, the model generalizes well to unseen categories better than EGM and STM. Among the models outperforming us, CFBI utilizes a stronger backbone, the recent KMN proposed a kernelized memory read and a pre-training trick which can be also added to our framework. KMN also has a linearly-growing memory, similar to STM.

4.1.3 Memory Analysis

We mentioned in Sec. 3.2 variants for updating the memory. To evaluate which one is the most efficient we test our model on the DAVIS 2017 validation set. The results are showed in table 4. We observe that the results of **C** and **D** are much better than those of **A** and **B**. This can be explained that using one template to update/enhance all the others can create too much overlapped information. In the worst case, if the chosen template contains errors, these errors will be spread out over the whole memory.

Additionally, by choosing the least similar pair of templates to update, the model yields better performance than that of the model uses the most similar pair of template to update. This result goes against our intuition that the update process should be easier and more effective given that the information of 2 templates is more similar and also maintain a more diverse memory by removing duplicate information. One possible explanation is that by choosing the least similar pair of templates (i.e. (i, j) such that $i < j$), we also add a prior which encourages the to regularly remove outdated information that are significantly different from other appearances from the memory.

Additionally, we mention earlier that instead of using the input to update directly, the memory will allows internal interaction among different memory templates. We conduct an experiment and show the results in Tab. 3. It shows that our update rule that always remembers the latest frame is significantly better than that of LSTM and NTM.

Method	Backbone	Memory size	Validation			Test-dev		
			J	F	Avg	J	F	Avg
LWL (OL) [2]	Resnet 50	N/A	72.2	76.3	74.3	-	-	-
PReMVOS (OL) [18]	Resnet 101	N/A	73.9	81.7	77.8	67.5	75.7	71.6
FEELVOS [26]	DeepLab v3	N/A	65.9	72.3	69.1	-	-	-
STM [20]	Resnet 50	linear growth	69.2	74.0	71.6	-	-	-
KMN [23]	Resnet 50	linear growth	74.2	77.8	76.0	-	-	-
CFBI [35]	Resnet 101	N/A	72.1	77.7	74.9	-	-	-
GC [14]	Resnet 50	constant	69.3	73.5	71.4	-	-	-
Ours	Resnet 50	constant	76.1	81	78.5	66.2	73.1	69.7

Table 1. The quantitative comparison on DAVIS 2017 val and test-dev set with other methods that are only trained or fine-tuned on DAVIS 2017. **OL**: online learning. **N/A**: not a memory-based method.



Figure 5. Qualitative results. (Best viewed in color)

4.1.4 Qualitative Results

In Fig. 5 and Fig. 6, we show some qualitative results on Davis 2017 dataset. The results show that our model is able to capture a variety of object poses, maintain a long-term memory after occlusion, and adapt well to most of the appearance change. However, in some extreme cases where the objects are too small or blurry, our model fails to capture the correct features for them. These cases suggest that we need to provide a dedicated module to handle multi-scale objects and a motion model to better segment the objects instead of only basing on the appearance model.

4.2. Video prediction

In this task, we compare our model with other memory architectures on the video prediction task. The overall architecture and memory management strategy is unchanged. Besides, because we no longer need to extract object-specific features, we can remove the query encoder. The backbones for the encoder and the decoder are scaled down to only 6 convolutional and deconvolutional layers respectively. Our approach outperforms others on MSE, MAE, and SSIM - Tab.5.

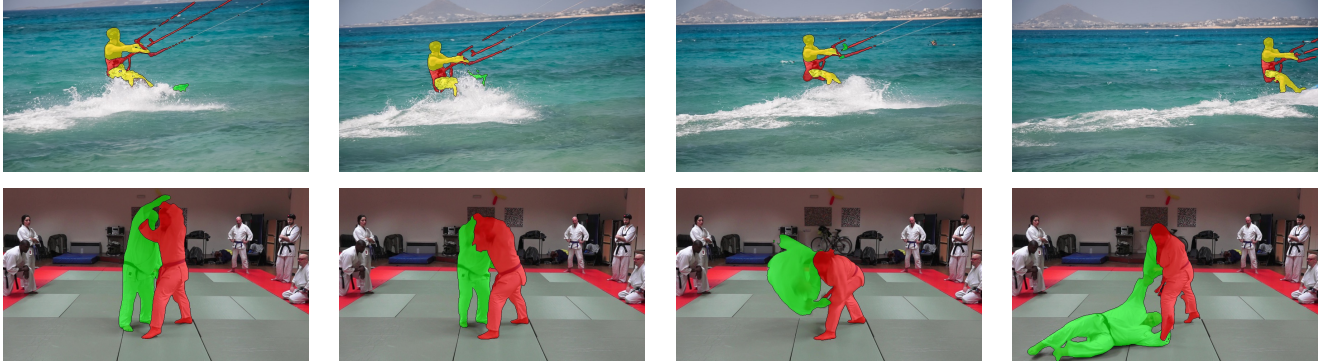


Figure 6. Failure cases. (Best viewed in color)

Methods	Seen		Unseen		Avg
	J	F	J	F	
GC(R50) [14]	72.6	75.6	68.9	75.7	73.2
EGM(R50) [17]	80.7	85.1	74.0	80.9	80.2
CFBI(R101) [35]	81.1	85.8	75.3	83.4	81.4
PReMVOS(R101) [18]	71.4	75.9	56.5	63.7	66.9
A-Game(R101) [10]	67.8	-	60.8	-	66.1
KMN (R50) [23]	81.4	85.6	72.8	84.2	80.9
STM(R50) [20]	79.7	84.2	72.8	80.9	79.4
Ours	77.2	81.1	73.4	82.4	78.5
STM(R50, -Y) [20]	-	-	-	-	56.3
Ours (-Y)	71.4	75.3	61.9	69.5	69.6

Table 2. Results on Youtube VOS 2018 validation set. (-Y): the model is only fine-tuned on DAVIS and tested directly on Youtube.

R50/101: use resnet 50/101 as backbone.

Methods	J	F	Avg
Input to memory (I2M)	69.2	74.7	72.0
Memory to memory (M2M)	76.1	81.0	78.5

Table 3. The I2M model uses the new template to update current memory cells. In contrast, the M2M model uses another memory cell to update current cells. Both models are evaluated on Davis 2017 validation set.

Memory variants	J	F	Mean
Oldest vs remaining (A)	74.5	80.1	77.3
Latest vs remaining (B)	73.0	78.5	75.7
Least similarity pair (C)	76.1	81.0	78.5
Most similarity pair (D)	74.9	80.1	77.5

Table 4. Results on DAVIS 2017 validation set for different memory update strategies.

5. Conclusion

In this paper, we proposed a novel memory network architecture with the potential for scaling up to long videos. We test multiple memory update strategies and choose the one that allows the interactions among memory cells. This allows our model to reason on high order information of

Method	Human 3.6		
	MSE/10	MAE/100	SSIM
ConvLSTM [25]	50.4	18.9	0.776
PredRNN [30]	48.4	18.9	0.781
Causal LSTM [28]	45.8	17.2	0.851
MIM [31]	42.9	17.8	0.79
E3D-LSTM [29]	46.4	16.6	0.869
Ours	37.04	14.23	0.905

Table 5. Video prediction results

past frames. Finally, we showed that our model worked well on VOS, which is a complex task, and achieved the best result on the DAVIS 2017 validation set (when trained only on synthetic data and DAVIS) and competitive results on Youtube VOS. Our results on the video prediction also show that our memory architecture has a huge potential to extend to tasks that require long term memory. In the future, we hope that our model can be extended to other tasks such as video reasoning, reinforcement learning, and embodied AI.

References

- [1] Linchao Bao, Baoyuan Wu, and Wei Liu. Cnn in mrf: Video object segmentation via inference in a cnn-based higher-order spatio-temporal mrf. In *Proceedings of the IEEE conference on computer vision and pattern recognition*, pages 5977–5986, 2018. 3
- [2] Goutam Bhat, Felix Järemo Lawin, Martin Danelljan, Andreas Robinson, Michael Felsberg, Luc Van Gool, and Radu Timofte. Learning what to learn for video object segmentation. In *European Conference on Computer Vision*, pages 777–794. Springer, 2020. 3, 7
- [3] Sergi Caelles, Kevis-Kokitsi Maninis, Jordi Pont-Tuset, Laura Leal-Taixé, Daniel Cremers, and Luc Van Gool. One-shot video object segmentation. In *Proceedings of the IEEE conference on computer vision and pattern recognition*, pages 221–230, 2017. 3
- [4] M. Cheng, N. J. Mitra, X. Huang, P. H. S. Torr, and S. Hu. Global contrast based salient region detection. *IEEE*

- Transactions on Pattern Analysis and Machine Intelligence*, 37(3):569–582, 2015. 5
- [5] Alex Graves, Greg Wayne, and Ivo Danihelka. Neural Turing machines. *CoRR*, abs/1410.5401, 2014. 2, 5
- [6] Bharath Hariharan, Pablo Arbelaez, Lubomir Bourdev, Subhransu Maji, and Jitendra Malik. Semantic contours from inverse detectors. In *International Conference on Computer Vision (ICCV)*, 2011. 5
- [7] Sepp Hochreiter and Jürgen Schmidhuber. Long short-term memory. *Neural computation*, 9(8):1735–1780, 1997. 2, 5
- [8] Yuan-Ting Hu, Jia-Bin Huang, and Alexander G Schwing. Maskrcnn: Instance level video object segmentation. *arXiv preprint arXiv:1803.11187*, 2018. 3
- [9] Sergey Ioffe and Christian Szegedy. Batch normalization: Accelerating deep network training by reducing internal covariate shift. In *International conference on machine learning*, pages 448–456. PMLR, 2015. 5
- [10] Joakim Johnander, Martin Danelljan, Emil Brissman, Fahad Shahbaz Khan, and Michael Felsberg. A generative appearance model for end-to-end video object segmentation. In *Proceedings of the IEEE/CVF Conference on Computer Vision and Pattern Recognition (CVPR)*, June 2019. 8
- [11] Chanho Kim, Fuxin Li, and James M Rehg. Multi-object tracking with neural gating using bilinear lstm. In *Proceedings of the European Conference on Computer Vision (ECCV)*, pages 200–215, 2018. 2
- [12] G. Li and Y. Yu. Visual saliency based on multiscale deep features. In *IEEE Conference on Computer Vision and Pattern Recognition (CVPR)*, pages 5455–5463, June 2015. 5
- [13] Xiaoxiao Li and Chen Change Loy. Video object segmentation with joint re-identification and attention-aware mask propagation. In *Proceedings of the European Conference on Computer Vision (ECCV)*, pages 90–105, 2018. 3
- [14] Yu Li, Zhuoran Shen, and Ying Shan. Fast video object segmentation using the global context module. In Andrea Vedaldi, Horst Bischof, Thomas Brox, and Jan-Michael Frahm, editors, *Computer Vision - ECCV 2020 - 16th European Conference, Glasgow, UK, August 23-28, 2020, Proceedings, Part X*, volume 12355 of *Lecture Notes in Computer Science*, pages 735–750. Springer, 2020. 2, 4, 7, 8
- [15] Huaijia Lin, Xiaojuan Qi, and Jiaya Jia. Agss-vos: Attention guided single-shot video object segmentation. In *Proceedings of the IEEE/CVF International Conference on Computer Vision*, pages 3949–3957, 2019. 4
- [16] Tsung-Yi Lin, Michael Maire, Serge Belongie, James Hays, Pietro Perona, Deva Ramanan, Piotr Dollár, and C Lawrence Zitnick. Microsoft coco: Common objects in context. In *European conference on computer vision*, pages 740–755. Springer, 2014. 5
- [17] Xiankai Lu, Wenguan Wang, Danelljan Martin, Tianfei Zhou, Jianbing Shen, and Van Gool Luc. Video object segmentation with episodic graph memory networks. In *ECCV*, 2020. 2, 8
- [18] Jonathon Luiten, Paul Voigtlaender, and Bastian Leibe. Premvos: Proposal-generation, refinement and merging for video object segmentation. In *Asian Conference on Computer Vision*, 2018. 7, 8
- [19] Seoung Wug Oh, Joon-Young Lee, Kalyan Sunkavalli, and Seon Joo Kim. Fast video object segmentation by reference-guided mask propagation. In *Proceedings of the IEEE conference on computer vision and pattern recognition*, pages 7376–7385, 2018. 4
- [20] Seoung Wug Oh, Joon-Young Lee, Ning Xu, and Seon Joo Kim. Video object segmentation using space-time memory networks. In *Proceedings of the IEEE/CVF International Conference on Computer Vision (ICCV)*, October 2019. 1, 2, 4, 5, 7, 8
- [21] Federico Perazzi, Anna Khoreva, Rodrigo Benenson, Bernt Schiele, and Alexander Sorkine-Hornung. Learning video object segmentation from static images. In *Proceedings of the IEEE conference on computer vision and pattern recognition*, pages 2663–2672, 2017. 3
- [22] Andreas Robinson, Felix Jaremo Lawin, Martin Danelljan, Fahad Shahbaz Khan, and Michael Felsberg. Learning fast and robust target models for video object segmentation. In *Proceedings of the IEEE/CVF Conference on Computer Vision and Pattern Recognition*, pages 7406–7415, 2020. 3
- [23] Hongje Seong, Junhyuk Hyun, and Euntai Kim. Kernelized memory network for video object segmentation. In *European Conference on Computer Vision*, pages 629–645. Springer, 2020. 4, 7, 8
- [24] Xingjian SHI, Zhourong Chen, Hao Wang, Dit-Yan Yeung, Wai-kin Wong, and Wang-chun WOO. Convolutional lstm network: A machine learning approach for precipitation nowcasting. In C. Cortes, N. Lawrence, D. Lee, M. Sugiyama, and R. Garnett, editors, *Advances in Neural Information Processing Systems*, volume 28, pages 802–810. Curran Associates, Inc., 2015. 2
- [25] Xingjian Shi, Zhourong Chen, Hao Wang, Dit Yan Yeung, Wai Kin Wong, and Wang Chun Woo. Convolutional lstm network: A machine learning approach for precipitation nowcasting. *Advances in neural information processing systems*, 2015:802–810, 2015. 8
- [26] P. Voigtlaender, Yuning Chai, Florian Schroff, H. Adam, B. Leibe, and Liang-Chieh Chen. Feelvos: Fast end-to-end embedding learning for video object segmentation. *2019 IEEE/CVF Conference on Computer Vision and Pattern Recognition (CVPR)*, pages 9473–9482, 2019. 7
- [27] Paul Voigtlaender and Bastian Leibe. Online adaptation of convolutional neural networks for the 2017 davis challenge on video object segmentation. In *The 2017 DAVIS Challenge on Video Object Segmentation-CVPR Workshops*, volume 5, 2017. 3
- [28] Yunbo Wang, Zhifeng Gao, Mingsheng Long, Jianmin Wang, and S Yu Philip. Predrnn++: Towards a resolution of the deep-in-time dilemma in spatiotemporal predictive learning. In *International Conference on Machine Learning*, pages 5123–5132. PMLR, 2018. 8
- [29] Yunbo Wang, Lu Jiang, Ming-Hsuan Yang, Li-Jia Li, Mingsheng Long, and Li Fei-Fei. Eidetic 3d lstm: A model for video prediction and beyond. In *International conference on learning representations*, 2018. 8
- [30] Yunbo Wang, Mingsheng Long, Jianmin Wang, Zhifeng Gao, and Philip S Yu. Predrnn: Recurrent neural networks

- for predictive learning using spatiotemporal lstms. In *Proceedings of the 31st International Conference on Neural Information Processing Systems*, pages 879–888, 2017. 8
- [31] Yunbo Wang, Jianjin Zhang, Hongyu Zhu, Mingsheng Long, Jianmin Wang, and Philip S Yu. Memory in memory: A predictive neural network for learning higher-order non-stationarity from spatiotemporal dynamics. In *Proceedings of the IEEE/CVF Conference on Computer Vision and Pattern Recognition*, pages 9154–9162, 2019. 8
- [32] Yuxin Wu and Kaiming He. Group normalization. In *Proceedings of the European conference on computer vision (ECCV)*, pages 3–19, 2018. 5
- [33] Q. Yan, L. Xu, J. Shi, and J. Jia. Hierarchical saliency detection. *2013 IEEE Conference on Computer Vision and Pattern Recognition*, pages 1155–1162, 2013. 5
- [34] Linjie Yang, Yanran Wang, Xuehan Xiong, Jianchao Yang, and Aggelos K Katsaggelos. Efficient video object segmentation via network modulation. In *Proceedings of the IEEE Conference on Computer Vision and Pattern Recognition*, pages 6499–6507, 2018. 4
- [35] Zongxin Yang, Yunchao Wei, and Yi Yang. Collaborative video object segmentation by foreground-background integration. In *Proceedings of the European Conference on Computer Vision*, 2020. 4, 7, 8